fatigue, wheel tyre, Wohler diagram

Henryk BĄKOWSKI*, Piotr CZECH
Silesian University of Technology, Faculty of Transport
Krasińskiego 8, 40-019 Katowice, Poland
**Corresponding author*. E-mail: henryk.bakowski@polsl.pl

WEAR ESTIMATION OF THE WHEEL TYRE IN DIFFERENT SERVICE CONDITIONS

Summary. In this article presented the results of fatigue strength test aluminium alloys using in car industry. Demonstrated distributions and values of stresses the wheel tyre made of aluminium alloys by means of FEM. In fatigue test used special machine, which can allow to determine Wohler diagram. In this way to determine the allowable stresses values in which do not occurring the damages.

OCENA ZUŻYCIA OBRĘCZY KOŁA W RÓŻNYCH WARUNKACH EKSPLOATACJI

Streszczenie. W artykule przedstawiono wyniki badań wytrzymałości zmęczeniowej stopów aluminium wykorzystywanych w przemyśle samochodowym. Opisano rozkłady i wartości naprężeń obręczy kół ze stopów aluminium za pomocą Metody Elementów Skończonych. W badaniach zmęczeniowych użyto specjalnej maszyny, która pozwoliła na wyznaczenie wytrzymałości zmęczeniowej krzywą Wohlera. W ten sposób określono wartości naprężeń dopuszczalnych, przy których nie wystąpią uszkodzenia.

1. INTRODUCTION

The phenomenon of fatigue had been found at the beginning of the XXth century and one of the first to made attempt to understand and predict the fatigue damage was a German engineer August Wohler. He observed that the machine parts and constructions can be destroyed at a stress level much lower than the strength of the material, or even the yield stress. Hypothesized that the loss of load is caused by the cyclic loading and unloading structure. With the help of this machine has created a chart in which the strength of the material was dependent on the number of cycles. Constructions subjected to repeated dynamic loads are destroyed. Symptoms of damage are cracks occurring after a specified number of load changes. This type of wear is called fatigue. Fatigue cracks can be characterized by brittle cracks. They are very dangerous because the formation of fatigue cracks often remains unnoticed which means the destruction of suddenly, and unexpectedly, usually leads to dangerous failure. Studies have shown that about 80% of all cracks are caused by fatigue and a static load of only 20% [1]. In service conditions we can meet different damages (Fig. 1-2).

The important features that determine the applicability of the materials to build a set of machines and structures are mechanical properties. For this reason, the materials subjected to the tests of mechanical properties to determine the resistance of material to the load, and in some cases the effects of the environment. The most reflects the testing of materials under conditions close as possible for the machine or structure, which is not always realizable. Destruction of fatigue is one of the most commonly reported type of structural damage, and is extremely dangerous because it is unexpected. Fatigue occurs in the motor vehicle and parts, aircraft engines, generators and a number of other structures [2]. Fatigue is the result of loads, which varies in time. It become so important to determine the stress below which no fatigue damage occurs or specify the time during which it can lead to disaster. Course load is a random variable that results from the operation [3]. The cars will be the impact of rough roads, engine and chassis vibrations which imposes a charge distribution or maneuvering while driving (Fig. 1, 2) [7].

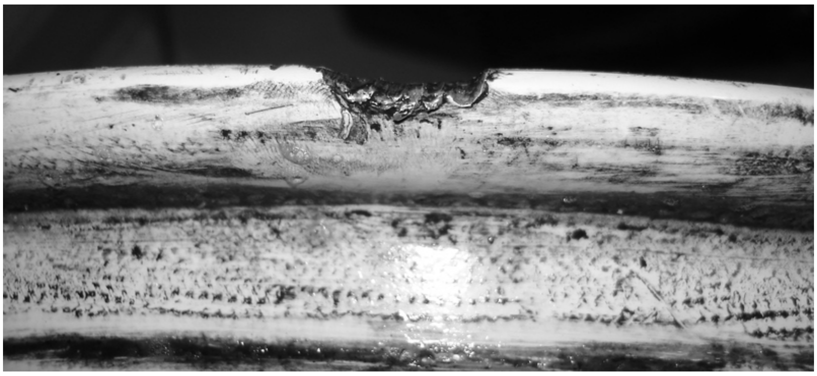

Fig. 1. Damage of the wheel tyre flange
Rys. 1. Uszkodzenie krawędzi obręczy koła

Fig. 2. Huge holes in the road
Rys. 2. Wielkie wyrwy w jezdni

The main objectives of the present study are:
- design and construction stand to fatigue strength test for both sides bending (Fig. 3-4),
- determination fatigue diagrams (Wöhler curves) for selected materials construction occurring in vehicles (Fig. 5-6),
- statistical, metallographic and numerical analysis of the test results on the basis of examinations (Fig. 7-12, Tab. 3-4).

2. MATERIALS AND EQUIPMENT

The important features that determine the applicability of materials for the construction of special machines and structures are mechanical properties. The study used two different materials such as aluminum alloy containing 5% silicon, and aluminum alloy containing 5% magnesium. Designations and properties of the materials compared presented in tables 1-2.

Table 1

Designations and properties of the aluminum alloy containing 5% silicon

Designation according to standards	
DIN 1732	SG AlSi 5
Werkstoff Numer	3.2245
PN – 75/M – 69414	SPA 26
B.S.2901,cz.4	4043 A
EN	AW 4043
AWS/ASME SFA	ER4043
Physical properties	
electrical conductivity at 20^0C	24-32 [s*m/mm^2]
thermal conductivity at 20^0C	170 [W/(m*K)]
coefficient of linear thermal expansion [20-100^0]	23,7x10^{-6} [1/K]
Mechanical strength values	
0,2% - yield strength $Rp_{0,2}$	100 [N/mm^2]
tensile strength R_m	160 [N/mm^2]
elongation A_5	15 [%]

Table 2

Designations and properties of the aluminum alloy containing 5% magnesium

Designation according to standards	
DIN 1732	SG AlMg 5
Werkstoff Numer	3.3556
PN – 75/M – 69414	SPA
B.S.2901,cz.4	5056 A
EN	AW 5056
AWS/ASME SFA	ER 5356
Physical properties	
electrical conductivity at 20^0C	15 - 19 [s*m/mm^2]
thermal conductivity at 20^0C	110 – 150 [W/(m*K)]
coefficient of linear thermal expansion [20-100^0]	23,7x10^{-6} [1/K]
Mechanical strength values	
0,2% - yield strength $Rp_{0,2}$	110 [N/mm^2]
tensile strength R_m	250 [N/mm^2]
elongation A_5	25 [%]

The device which is designed and built to test the fatigue strength of non-ferrous metals mainly aluminum alloys. The test samples are subjected to pulsating loads at both ends of pure bending. Laboratory experiments has been carried out on both sides bending [6]. Fig. 3 and 4 presents a view of the device.

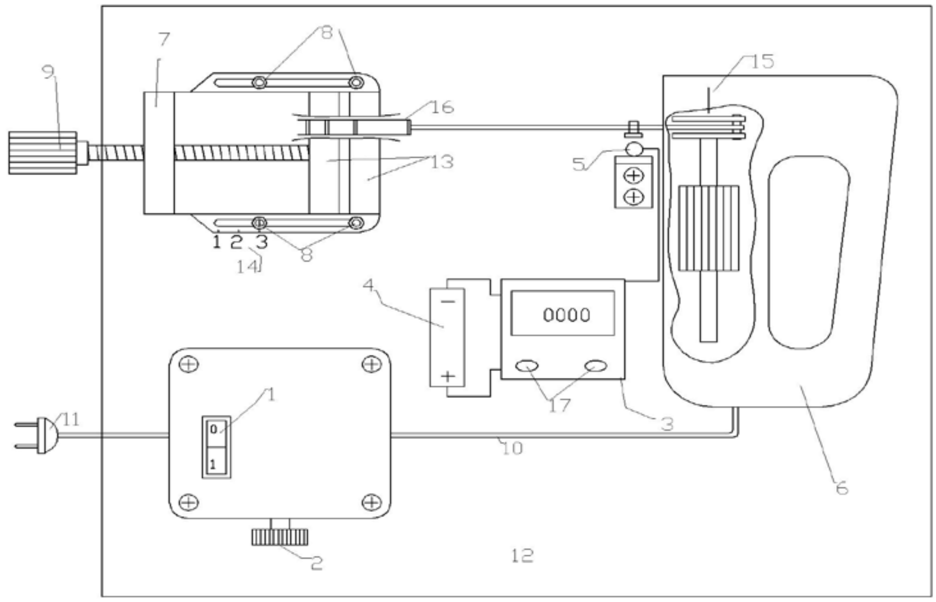

Fig. 3. View from the top of the unit: (1) switch, (2) the speed controller AVT 1007, (3) bike computer, (4) ports supply battery meter, (5) the sensor meter (6) device that produces a reciprocating motion-turning driven commutator motor (Jig), (7) vice modeling, (8) screws to set the vices, (9) adjustable jaw vise (10) electric wire (11) AC power plug, (12) plate (13) of vice modeling, (14) the timing marks vices, (15) sign positioner machine (16) arm with three notches (17) counter function keys. The main parts of the machine are attached to the plate (12): a device producing a reciprocating motion-turning (6), vice Models (7) counter (3) with the socket on the battery that supplies power meter (4), the switch (1) and speed controller (2)

Rys. 3. Widok z góry urządzenia: (1) włącznik, (2) regulator prędkości obrotowej AVT 1007, (3) licznik rowerowy, (4) gniazdo na baterię zasilającą licznik, (5) czujnik licznika, (6) urządzenie wytwarzające ruch posuwisto-zwrotny napędzane silnikiem komutatorowym (wyrzynarka), (7) imadło modelarskie, (8) śruby do ustawiania imadła, (9) regulacja szczęk imadła, (10) przewód elektryczny, (11) wtyczka zasilająca AC, (12) płyta, (13) szczęki imadła modelarskiego, (14) znaki ustawcze imadła, (15) znak ustawczy maszyny, (16) ramię z trzema wycięciami, (17) przyciski funkcyjne licznika. Główne części maszyny przymocowane są do płyty (12): urządzenie wytwarzające ruch posuwisto-zwrotny (6), imadło modelarskie (7), licznik (3) wraz z gniazdem na baterię zasilającą licznik (4), włącznik (1) oraz regulator prędkości obrotowej (2)

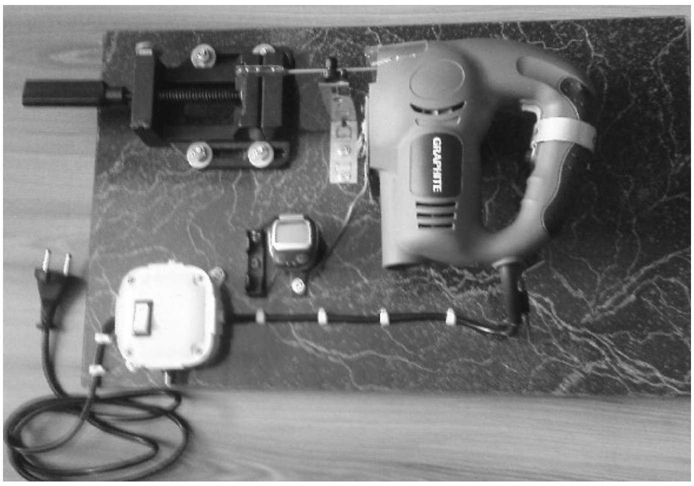

Fig. 4. General view of the machine
Rys. 4. Widok ogólny maszyny

3. RESEARCH RESULTS

The results of the tests have been presented in Table 3, 4 and on Figure 5, 6.

Table 3

Statement of the results and statistical values for the alloy AlSi 5

Numbers	Deflection [m]	Stress σ [MPa]	σ^2	Number of cycles N	lg N	lg^2N	σ * lg N
1	0,0075	1763,27	3109105	40	1,6021	2,5666	2824,8568
2	0,0075	1763,27	3109105	38	1,5798	2,4957	2785,5776
3	0,0075	1763,27	3109105	41	1,6128	2,6011	2843,7658
4	0,0032	752,33	565995,2	61	1,7853	3,1874	1343,1510
5	0,0032	752,33	565995,2	64	1,8062	3,2623	1358,8371
6	0,0032	752,33	565995,2	52	1,7160	2,9447	1290,9948
7	0,0024	564,24	318372,3	175	2,2430	5,0312	1265,6228
8	0,0024	564,24	318372,3	151	2,1790	4,7479	1229,4766
9	0,0024	564,24	318372,3	137	2,1367	4,5656	1205,6337
Suma Σ	-	9239,51	11980416	-	16,6609	31,4025	16147,9163

Table 4

Statement of the results and statistical values for the alloy AlMg 5

Numbers	Deflection [m]	Stress σ [MPa]	σ^2	Number of cycles N	lg N	lg^2N	σ * lg N
1	0,0075	1564,90	2448906	85	1,9294	3,7227	3019,3437
2	0,0075	1564,90	2448906	92	1,9638	3,8565	3073,1276
3	0,0075	1564,90	2448906	75	1,8751	3,5159	2934,2795
4	0,0032	667,69	445809,7	160	2,2041	4,8581	1471,6684
5	0,0032	667,69	445809,7	135	2,1303	4,5383	1422,4021
6	0,0032	667,69	445809,7	142	2,1523	4,6323	1437,0610
7	0,0024	500,77	250767,9	401	2,6031	6,7764	1303,5697
8	0,0024	500,77	250767,9	370	2,5682	6,5957	1286,0716
9	0,0024	500,77	250767,9	420	2,6232	6,8814	1313,6376
Suma Σ	-	8200,065	9436450	-	20,0496	45,3772	17261,1612

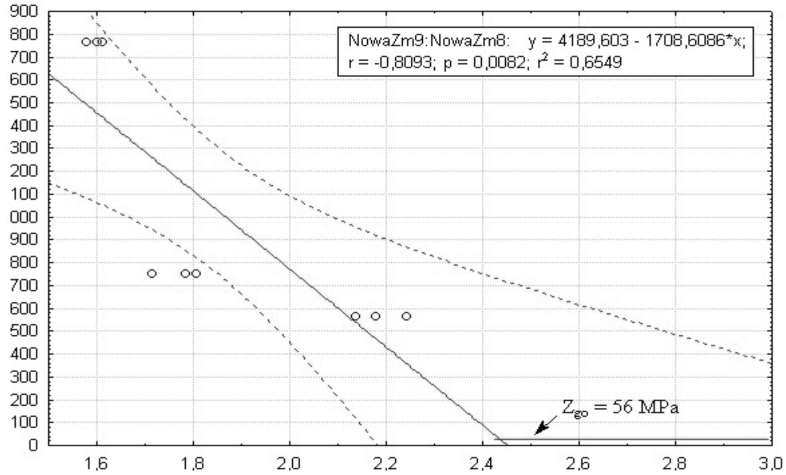

Fig. 5. Wohler diagram for aluminium alloy containing 5% silicon
Rys. 5. Wykres Wohlera dla stopu aluminium z 5% zawartością krzemu

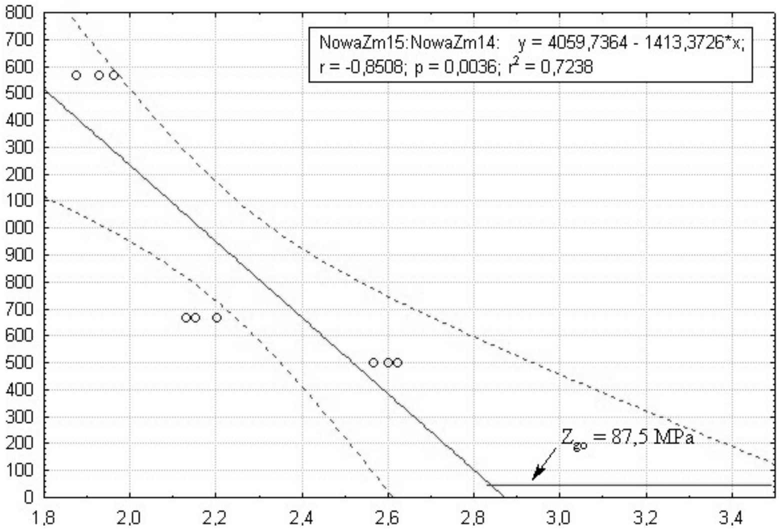

Fig. 6. Wohler diagram for aluminium alloy containing 5% magnesium
Rys. 6. Wykres Wohlera dla stopu aluminium z 5% zawartością magnezu

The metallographic examination of these specimens on metallographic microscope has been carried out (Fig. 7-11).

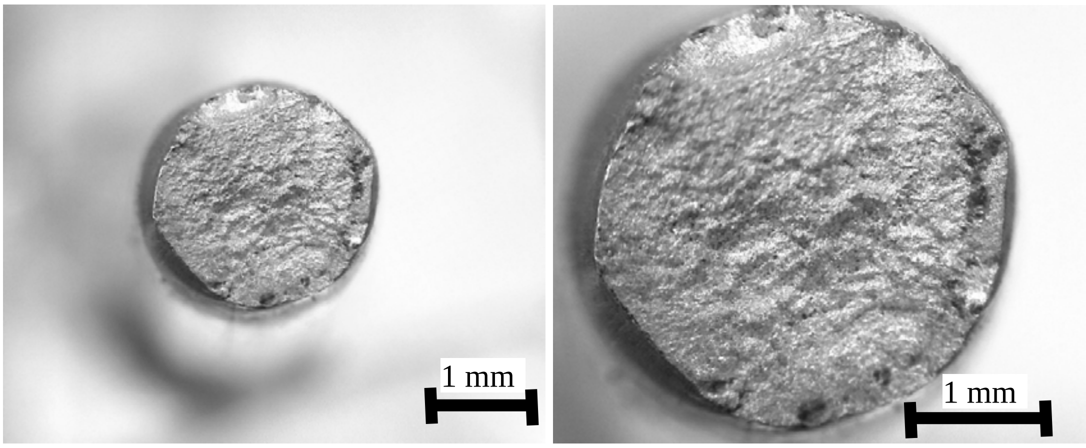

Fig. 7. Fatigue fracture of aluminum alloy containing 5% silikon for σ = 1763.2 MPa
Rys. 7. Przełom zmęczeniowy aluminium z 5% zawartością krzemu dla σ = 1763,2 MPa

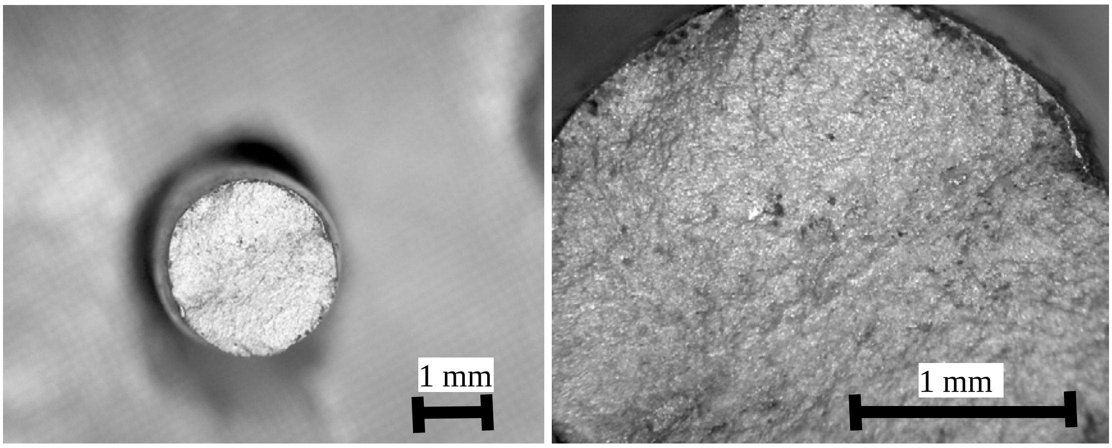

Fig. 8. Fatigue fracture of aluminum alloy containing 5% silikon for σ = 752.3 MPa
Rys. 8. Przełom zmęczeniowy aluminium z 5% zawartością kremu dla σ = 752,3 MPa

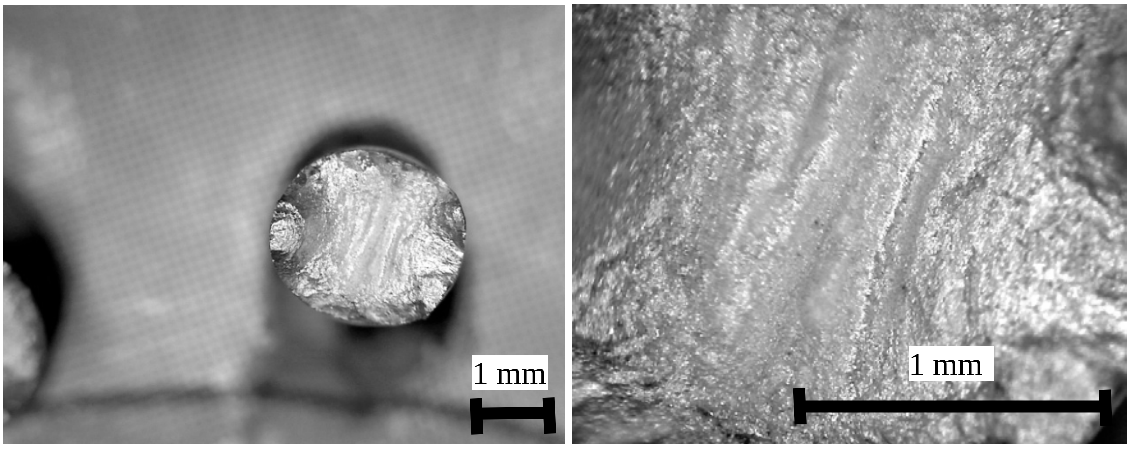

Fig. 9. Fatigue fracture of aluminum alloy containing 5% magnesium for σ = 1564.9 MPa
Rys. 9. Przełom zmęczeniowy aluminium z 5% zawartością magnezu dla σ = 1564,9 MPa

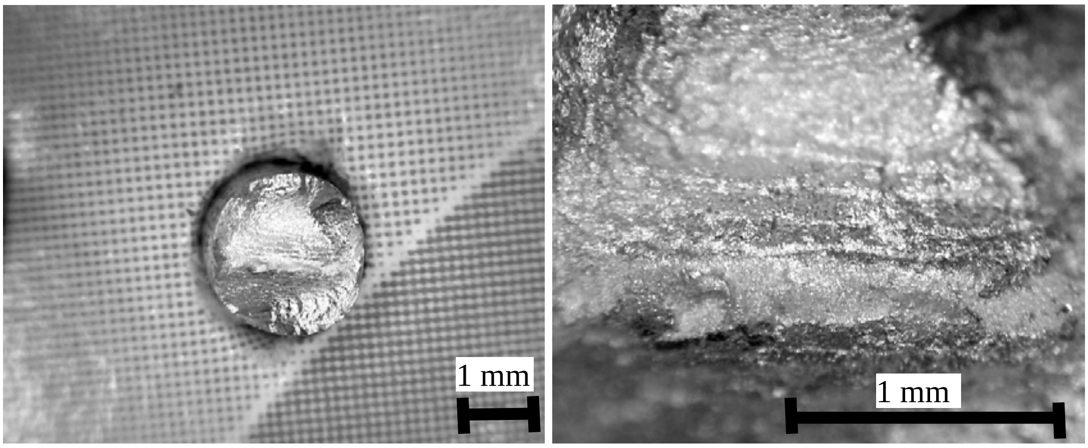

Fig. 10. Fatigue fracture of aluminum alloy containing 5% magnesium for σ = 667.7 MPa
Rys. 10. Przełom zmęczeniowy aluminium z 5% zawartością magnezu dla σ = 667,7 MPa

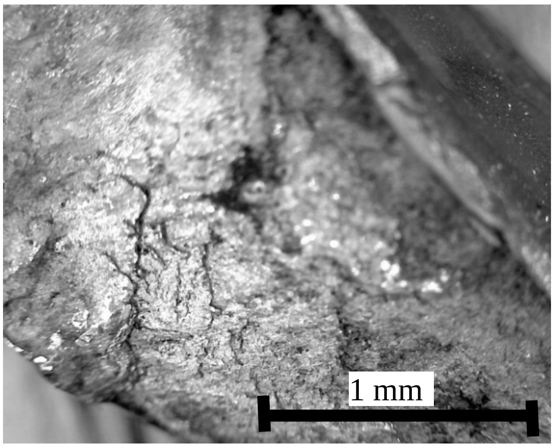

Fig. 11. Fatigue fracture of real object (wheel tyre)
Rys. 11. Przełom zmęczeniowy w obiekcie rzeczywistym (obręcz koła)

The simulations by means of FEM allowed determining the distributions of stress and finding the most dangerous places in which may occure damages (Fig. 12).

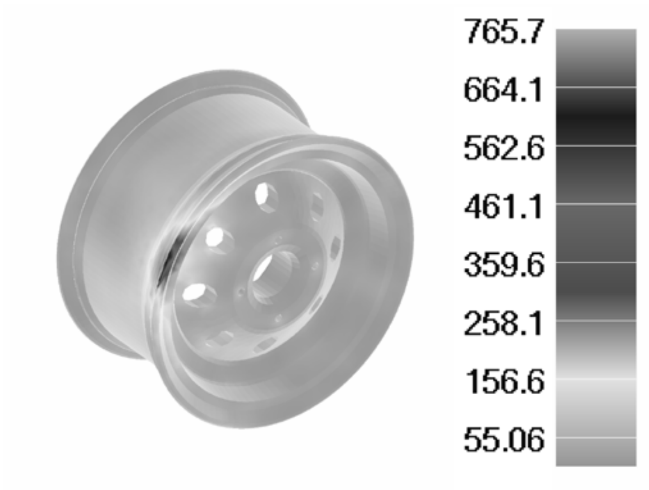

Fig. 12. Distribution of stresses (MPa) for wheel tyre by means of FEM
Rys. 12. Rozkład naprężeń (MPa) za pomocą MES obręczy koła

4. CONCLUSIONS

On the basis of the results it was found that aluminum alloy with 5% magnesium content was characterized by the highest fatigue strength. The survey received considerable scatter reflecting the small number of samples. For finer control, had to carry out tests on samples of more normalized using a standard device. During the study noted the presence of a phenomenon which was to strengthen and sudden weakening of the material after a certain number of cycles. This phenomenon occurred during each of the tests for all materials. The reason for strengthening local work hardening of the material is formed by bending both sides. During metallographic examination could obtain information about the structure of castings, the heterogeneity of the material, internal discontinuities, non-metallic inclusions, plastic properties and characteristics of fracture (plastic, brittle, mixed). This information is very useful in the analysis of the turn. Based on the observation proves what kind of load caused the crash, and what was the process of destruction [4, 5].

On the basis of carried out researches, it can be concluded that:

- the most fatigue strength is reached by aluminium alloy with magnesium (AlMg5),
- the occurrence of a phenomena which were strengthening and the sudden weakening of the material after some number of cycles. This problem occurred during each test for all materials. The main reason was the local deformation of the material caused by bending both sides,
- what type of load caused the crash and what was the destruction process (dynamic or static).

References

1. Maciejny, A. *Kruchość Metali*. Katowice: Wydawnictwo „Śląsk". 1973. 199 s. [In Polish: Maciejny, A. *Metals brittleness.* Katowice: Publishing house „Śląsk". 1973. 199 p.]
2. Kocańda, S. & Szala, J. *Podstawy obliczeń zmęczeniowych.* Warszawa: PWN. 1997. 288 s. [In Polish: Kocańda, S. & Szala, J. *The bases for calculating of fatigue*. Warszawa: PWN. 1997. 288 p.]
3. Kocańda, S. *Zmęczeniowe pękanie metali*. Warszawa: WNT. 1995. 441 p. [In Polish: Kocańda, S. *Fatigue cracking of metals.* Warszawa: WNT. 1995. 441 p.]
4. Topac, M.M. & Ercan, S. & Kuralay, N.S. Fatigue life prediction of a heavy vehicle steel wheel under radial loads by using Finite Element Analysis. *Engineering Failure Analysis*. 2012. No. 20. P. 67-79.

5. Firat, M. & Kozan, R. & Ozsoy, M. & Mete, O.H. Numerical modeling and simulation of wheel radial fatigue tests. *Engineering Failure Analysis*. 2009. No. 16. P. 1533-1541.
6. PN-EN 1999-1-3:2011/A1:2012P. *Projektowanie konstrukcji aluminiowych*. Available at: http://sklep.pkn.pl/pn-en-1999-1-3-2011-a1-2012p.html [In Polish: PN-EN 1999-1-3:2011/A1:2012P. Design of aluminum structures]
7. Łukaszewicz, A. *Jak dostać odszkodowanie za dziurę w jezdni*. Available at: http://prawo.rp.pl/galeria/757705,1,437906.html [In Polish: Lukaszewicz, A. How to get compensation for the hole in the road]

Received 23.11.2011; accepted in revised form 14.05.2014